Title

Congenital and acquired mandibular asymmetry: Mapping growth and remodeling in 3 dimensions

Journal

American Journal of Orthodontics and Dentofacial Orthopedics, 150(2)

ISSN

0889-5406

Authors

Solem, R Christian
Ruellas, Antonio
Ricks-Oddie, Joni L
et al.

Publication Date

2016-08-01

DOI

10.1016/j.ajodo.2016.02.015

Peer reviewed

HHS Public Access

Author manuscript

Am J Orthod Dentofacial Orthop. Author manuscript; available in PMC 2016 October 04.

Published in final edited form as:

Am J Orthod Dentofacial Orthop. 2016 August ; 150(2): 238–251. doi:10.1016/j.ajodo.2016.02.015.

Congenital and acquired mandibular asymmetry: Mapping growth and remodeling in 3 dimensions

R. Christian Solem[a] **[Lecturer]**, **Antonio Ruellas**[b] **[Associate professor]**, **Arthur Miller**[c] **[Professor]**, **Katherine Kelly**[d] **[Adjunct clinical assistant professor]**, **Joni L. Ricks-Oddie**[e] **[Statistical consultant]**, and **Lucia Cevidanes**[f] **[Assistant professor]**

[a]Section of Orthodontics, University of California, Los Angeles, Calif

[b]Federal University of Rio de Janerio, Rio de Janerio, Brazil; postdoctoral fellow, School of Dentistry, University of Michigan, Ann Arbor, Mich

[c]School of Dentistry, University of California, San Francisco, Calif

[d]Department of Orthodontics and Pediatric Dentistry, School of Dentistry, University of Michigan, Ann Arbor, Mich

[e]Institute for Digital Research and Education, University of California, Los Angeles, Calif

[f]Department of Orthodontics and Pediatric Dentistry, School of Dentistry, University of Michigan, Ann Arbor, Mich

Abstract

Introduction—Disordered craniofacial development frequently results in definitive facial asymmetries that can significantly impact a person's social and functional well-being. The mandible plays a prominent role in defining facial symmetry and, as an active region of growth, commonly acquires asymmetric features. Additionally, syndromic mandibular asymmetry characterizes craniofacial microsomia (CFM), the second most prevalent congenital craniofacial anomaly (1:3000 to 1:5000 live births) after cleft lip and palate. We hypothesized that asymmetric rates of mandibular growth occur in the context of syndromic and acquired facial asymmetries.

Methods—To test this hypothesis, a spherical harmonic-based shape correspondence algorithm was applied to quantify and characterize asymmetries in mandibular growth and remodeling in 3 groups during adolescence. Longitudinal time points were automatically registered, and regions of the condyle and posterior ramus were selected for growth quantification. The first group (n = 9) had a diagnosis of CFM, limited to Pruzansky-Kaban type I or IIA mandibular deformities. The second group (n = 10) consisted of subjects with asymmetric, nonsyndromic dentofacial asymmetry requiring surgical intervention. A control group (n = 10) of symmetric patients was selected for comparison. A linear mixed model was used for the statistical comparison of growth asymmetry between the groups.

Address correspondence to: R. Christian Solem, UCLA School of Dentistry, CHS 30-121, 10833 Le Conte Ave, Los Angeles, CA 90095; rchristian@g.ucla.edu.

All authors have completed and submitted the ICMJE Form for Disclosure of Potential Conflicts of Interest, and none were reported.

Results—Initial mandibular shape and symmetry displayed distinct signatures in the 3 groups ($P < 0.001$), with the greatest asymmetries in the condyle and ramus. Similarly, mandibular growth had unique patterns in the groups. The dentofacial asymmetry group was characterized by significant asymmetry in condylar and posterior ramal remodeling with growth ($P < 0.001$). The CFM group was characterized by asymmetric growth of the posterior ramus ($P < 0.001$) but relatively symmetric growth of the condyles ($P = 0.47$).

Conclusions—Forms of CFM are characterized by active and variable growth of the dysplastic side, which has a distinct pattern from other disorders of mandibular growth.

The mandible is the primary moving and functioning bone in the craniofacial skeleton and consequently plays a central role in defining facial morphology and symmetry. In active regions of growth, dysplasia during childhood can lead to severe facial deformity. Asymmetric mandibular growth occurs in the context of a diverse set of congenital and acquired conditions, including craniofacial microsomia (CFM) and hemimandibular hyperplasia or hypertrophy. The unpredictable nature of asymmetric growth, often affecting symmetry in all 3 planes of space, creates a particular challenge for planning surgical and orthodontic treatment strategies. CFM is the second most common congenital craniofacial anomaly after cleft lip and palate, occurring in 1:3000 to 1:5000 live births.[1–3] Derivatives of the first and second branchial arches are affected in a unilateral pattern. Thus, skeletal, neuromuscular, and other soft tissue components are affected. To a varying extent, these may include the ear, mandibular ramus, condyle, glenoid fossa, and associated muscles and nerves. Additionally, ocular, renal, spinal, and cardiac involvements may be present. Disruptions of cranial neural crest cell migration or proliferation during development are strongly implicated as potential etiologic factors.[4]

Disordered mandibular growth can be broadly categorized based on etiology as (1) congenital disorders of development, (2) primary growth disorders, and (3) disorders related to acquired trauma or disease.[5] The growth patterns in CFM are complex, involving all 3 planes of space.[1–3,6] In some patients, the affected side shows less growth relative to the unaffected side, whereas in others, there is significant compensatory growth. The associated neuromuscular derivatives are also affected to varying degrees and tend to grow less than the contralateral side.[3] In severe cases (types IIB and III of CFM[7]), the absence of structures important to growth, including condyle, ramus, and masticatory muscles, results in greatly diminished growth on the affected side. However, in milder cases where these structures are present, growth of the affected side can parallel that of the contralateral side.[8] It is postulated that variations in muscle activity and function may contribute to differences in growth.[9,10] In contrast to congenitally acquired forms, mandibular asymmetry more commonly develops postnatally from a variety of potential causes, including inflammatory resorptive changes to the condyle, hyperplastic condylar growth, asymmetry of the cranial base, and trauma.[5,6,11,12] Although the resulting pattern of mandibular growth in these conditions may resemble CFM, accurate diagnosis of the underlying etiology is essential to anticipate future growth changes.

In spite of many well-designed longitudinal studies, the progressive component of asymmetric growth in CFM remains controversial.[13–18] The trajectory of future growth is

central to surgical treatment planning strategies in deciding between early vs late intervention. Some studies have demonstrated progressive deformity with age,[14] whereas others reported significant compensatory growth of the affected side.[8,15,19] Generally, the degree of severity or type of asymmetric morphology has not been shown to correlate with the growth pattern of the maxilla or the mandible.[16,17] Wide interindividual variability in growth patterns has been observed.[8,16,17] This heterogeneity in clinical presentation and observed growth patterns in CFM presents a challenge to treatment planning. Consequently, approaches to treatment vary among clinicians. Some advocate early surgical intervention to enhance mandibular growth and reduce dysplastic compensatory growth.[13,14,20–22] Others prefer to minimize early surgical intervention and perform definitive correction near the completion of growth.[8,15–17,23] This viewpoint rests on evidence that shows significant growth of the affected side occurring in parallel with the contralateral side.[8,16,17] Clearly. additional clinical data are necessary to resolve this uncertainty.

Treatment strategies to correct or intercept asymmetric jaw growth depend on understanding the patterns of growth in these conditions. In this study, we aimed to (1) characterize and quantify mandibular asymmetry in conditions of abnormal growth, specifically CFM and noncongenitally acquired mandibular asymmetry; (2) quantify and image mandibular growth and remodeling patterns in these groups; and (3) identify localized regions of asymmetric growth in the 3 groups.

MATERIAL AND METHODS

Patients were selected for the 3 groups based on inclusion criteria related to their initial diagnosis. Because of the rarity of the syndrome, a retrospective case-control approach was used. The control patients (group A) were obtained from an unrelated retrospective study of consecutively treated orthodontic patients from a private practice clinic in Ann Arbor, Mich. They had Angle Class I occlusion and symmetric midlines, and they had received no orthopedic treatment. The use of cone-beam computed tomography (CBCT) images in this prior study was reviewed by the institutional review board at the University of Michigan. Patients in the control group were matched by age, sex, and cervical vertebral maturation (CVM) stage to the subjects in groups B and C (Table I). Group B consisted of patients with moderate to severe nonsyndromic dentofacial asymmetry from the orthodontic clinic at the University of Michigan or the University of California, San Francisco. Patients with inflammatory or degenerative changes to the condyle were excluded. Protocols were reviewed by the institutional review boards at the University of Michigan and the University of California (number HUM00078815). All patients in this group had a diagnosis of unilateral mandibular hyperplasia, based on radiographic and clinical findings over time. Only patients with a skeletal midline deviation of 3 mm or greater relative to the midsagittal reference plane were included.[24] Time point T0 was obtained as part of the initial records for phase 1 or 2 orthodontic treatment before completion of mandibular growth. The second time point (T1) was selected from records taken just before orthognathic surgery.

In group C, 9 patients with CFM or oculo-auriculo-vertebral (OAV) spectrum disorder were identified retrospectively from records in the craniofacial clinic at the University of California under medical search headings for hemifacial microsomia, Goldenhar’s

syndrome, or OAV. In this group, patients who came to the orthodontic clinic within the last 9 years were identified from 2 CBCT images obtained before orthognathic surgery, with T0 at the initial records and T1 prior to surgery. The average time between T0 and T1 was 2.1 years, ranging from 6 to 40 months. Only patients with a Pruzansky-Kaban Class I or IIA mandible were included in this group.[25,26] Because of the rarity of this syndrome, 9 subjects met the defined inclusion criteria. This patient sample is summarized in Table I, including the initial diagnosis and the specific skeletal growth stage (CVM) at the start of orthodontic treatment.[27]

CBCT radiographs were taken using a 0.376-mm^3 voxel dimension with a 9-in spherical volume on a CBCT scanner (MercuRay; Hitachi, Tokyo, Japan). Segmentation of the mandibular images from the CBCT data was performed with free open-source software (ITK-SNAP; http://www.itksnap.org). Edge-finding algorithms in this software were used for boundary detection so that arbitrary voxel-intensity thresholds were not required for segmentation.

The mandibular registration approach used in this study aimed only to find relative (right to left) differences in mandibular growth and remodeling over time. The mandibular time points were registered using an automated, voxel-wise approach that incorporated a reference region as a target. These steps essentially involve isolating a target region of the mandibular symphysis for registration using the voxel-wise approach described by Nguyen et al.[28] This region is limited to the U-shaped portion of the symphysis mesial to the first molar, with the outer and inferior cortical borders and internal tooth buds removed. The mandibles are first closely approximated manually, followed by successive iterations of automated registrations on the target region until the 6 registration parameters (translation [components x, y, and z], roll, yaw, and pitch) converge. The CMF growing registration module in the free open-source software 3D Slicer (CMFreg extension module; www.slicer.org) was used for automated registration. The method error was evaluated by repeating mandibular registrations and observations of growth; they showed a combined error of 1 mm or less using the Bland-Altman method.[29] Previous human[30] and animal model[31] studies have also shown that the errors of 3-dimensional (3D) mandibular registrations range from 0.3 to 1.0 mm with similar conditions and voxel sizes.

Correspondence between points on the surfaces of the 3D models at the 2 time points was established using a spherical harmonic-based algorithm, whereby the shape of the mandibular surface was approximated with a spherical harmonic series.[32] This analysis requires that the surfaces have spherical topology; therefore, the mandibular volume was divided into 2 halves at the midline so that a spherical coordinate system could be used in each. Second, the surface was filled so that it was smooth and continuous. The spherical harmonic analysis algorithm was then applied to determine shape-based correspondence between 2192 points over the hemimandibular surfaces.

After subtracting the corresponding 3D surfaces distances, color-coded maps were used to identify the regions of greatest growth for each patient. These regions were then selected for regional measurement of growth (Fig 1). The quantification method in this study followed a novel approach developed using the Pick ’n Paint extension module in the 3DSlicer software

(www.slicer.org). This approach enabled the propagation of regional surface points to corresponding regions of shape across all time points and patients. Two regions of mesh points were selected on an arbitrary reference left hemimandible at the superior surface of the condyle and the posterior surface of the ramus on each side (Fig 1). A radius of surface mesh points was defined around a center, creating a specific region of shape on the surface. The radius was equal to 4 mesh points for the condylar region (Fig 1, *A*) and 5 points for the posterior border of the ramus (Fig 1, *B*). This region was then automatically propagated through the entire population of hemimandibles using shape correspondence mapping, so that the same anatomic region was compared within sides of the mandible and between subjects. As a result, the placement of arbitrary landmarks was not required for the measurement of regional growth. Distances between corresponding points on the T0 to T1 surfaces, consisting of 61 regional measurements at the condyle (Fig 1, *A*) and 91 along the posterior border of the ramus (Fig 1, *B*), were selected for statistical comparison in a linear mixed model.

To characterize initial asymmetry at T0, all right hemimandibles were reflected to create a left mirror image. This enabled shape-based comparison of the right and left sides. Asymmetry between the right and left sides was compared by superimposing the mirrored image of the mandible on itself (Fig 2, *B*) according to the method described by Alhadidi et al.[33] To align these surfaces, the mirror image was first manually approximated to the original mandible. Then a final automated voxel-wise registration step was performed using the previously described target region. The 95th percentile displacement in selected regions of the condyle, ramus, and symphysis (Fig 2, *A*) was chosen to represent regional asymmetry in each subject. These results were then compared across the samples at T0.

Statistical analysis

The 3 groups were tested for statistical differences in age and CVM stage using the Kruskal-Wallis test, a nonparametric analysis of variance (ANOVA). A post-hoc power analysis with information collected from the study participants estimated the power to be 84%. A linear mixed model was used to test for statistical differences in growth between sides and regions of the mandible in the 3 groups. The nature of the project necessitated that multiple growth measurements of the mandible be taken from each patient. An ordinary least squares or ANOVA model would be inappropriate in this case because of the violation of the independence assumption.[34] A linear mixed model accommodates the observed nonindependence of observations and provides unbiased estimates of the effects of interest. Analogous to a repeated-measures ANOVA, a linear mixed model allows for the variations in mandibular growth measurements to be estimated at 2 levels, within subjects and between subjects. Beyond independence, linear mixed models share many of the same assumptions as those governing ordinary least squares, including the assumption of normally distributed residuals.[35] The residuals estimated by the model were found to be approximately normally distributed. A software package (StataSE 13; StataCorp, College Station, Tex) was used for all statistical analyses.

RESULTS

The populations in the 3 groups described in Table I were comparable in terms of initial age, treatment length, and CVM stage. No statistically significant difference was found in the age at T0 among groups A, B, and C ($P = 0.99$). Similarly, no difference was seen at T1 among the groups ($P = 0.97$). The median CVM stage, using the 5-stage system, was between II and III at T0 in all 3 groups.[27] According to Baccetti et al,[27] mandibular growth velocity peaks in less than 1 year after CVM stage II, indicating active mandibular growth during the measured time interval. No significant difference in CVM stage or sex was found among the groups ($P = 0.825$ and $P = 0.45$, respectively).

The local left and right asymmetries in the anatomic regions of interest are shown in millimeters for each group in Figure 2, *A*. Group A had the least initial asymmetry, with less than a 3-mm discrepancy in shape between the right and left sides. Asymmetry was greatest at the condyles. Group B was characterized by both greater overall asymmetry at the condyles and greater variability than group A ($P = 0.001$). Group C was characterized by the greatest asymmetry ($P < 0.001$), with over 10 mm of shape discrepancy at the condyles and over 5 mm at the ramus. Superimposed overlays (representative subjects in Fig 2, *B*) showed primarily inferior and superior shape discrepancies at the condyles in the dentofacial asymmetry group, whereas the CFM group had primarily mediolateral deviations in the position of the ramus and inferosuperior deviations in the position of the condyle.

Regional measurements of mandibular growth in the control group are shown in Figure 3, depicting both the direction (Fig 3, *A*; *white overlay*) and the magnitude (Fig 3, *B*; *colored surface*) of changes to the mandibular surface over time. In this group, the articulating surface of the condyle and the sigmoid notch showed the greatest appositions in a predominantly superior and posterior direction, with a slight lateral component. The directions varied in orientation between subjects, with some characterized by more vertical growth. The lingual surface of the condylar neck showed the greatest resorptive remodeling, with net resorption extending toward the lingula. The lingual surface of the gonial angle was also characterized by resorption. The resorptive pattern varied over the lingual surfaces between subjects, concentrated over the submandibular fossa. The lingual surface of the superior ramus and the posterior aspect of the mylohyoid ridge were characterized by apposition (Fig 3, *D* and *F*; *orange*). The posterior border of the ramus also showed appositional growth, which was concentrated at the gonial angle. This appositional region transitioned to resorptive toward the superior aspect of the posterior ramus. The dental arch was also characterized by active vertical growth, with a direction ranging from superior to anterosuperior. The anterior border of the symphysis showed variable and minor resorption. In some subjects (Fig 3, *C*; *white overlay*), significant apposition occurred at pogonion and the anterior portion of the inferior border.

The growth rate of the condyles was symmetric in the controls, with a mean right-to-left difference of −1.8% ± 5.7% over the measured period of growth (Table II). No statistically significant difference in growth between sides was seen at either the condyle or the ramus.

Growth of the mandible in the dentofacial asymmetry group was asymmetric primarily in the ramal and condylar regions, with the hyperplastic side of the mandible at T0 becoming taller at the condyle and longer at the posterior border (Fig 4). Asymmetric growth differences displayed a statistically significant preference for the hyperplastic side (Table II). At the condyle, 20% greater growth occurred on the hyperplastic side (Table II; $P < 0.001$). Growth along the posterior border of the ramus was similarly asymmetric, with 38% greater growth measured on the hyperplastic side, significantly greater than the control group (Table II; $P < 0.001$). The overall rates of mandibular growth on the hyperplastic side were greater than the control group (Table II), indicating above average rates of growth. The direction of growth of the hyperplastic condyle was similar to the contralateral side (Fig 4, *A, C*, and *E*), growing in a posterior and superior direction and mirroring the contralateral side. The posterior ramus grew in a similar pattern, with growth differing primarily in magnitude rather than direction between sides.

Patients in group C displayed distinctly unique growth morphologies, ranging from strongly asymmetric (Fig 5, *A* and *B*) to symmetric (Fig 5, *E* and *F*) in magnitude. Those with a type IIA diagnosis had the greatest discrepancy in growth between sides, as shown in Figure 5, *A* and *B*. Growth showed the greatest difference over the posterior ramus, with the dysplastic side characterized by less apposition, indicated by the more orange-red color on the contralateral posterior ramus (Fig 5). This asymmetry in posterior ramus growth was significantly greater than in the control group in the statistical model (Table II). In contrast, condylar growth showed no significant difference in mean asymmetry compared with the control group (Fig 6). The degree of asymmetric condylar growth was similar in patients with types I and IIA CFM, with no discernable difference from the control group. No significant difference was detected in the mean growth rate of the condyle between sides (Fig 6 and Table II); however, the apposition rate at the posterior ramus was 1.0 mm per year less on the dysplastic side.

In addition to the asymmetry in growth rate, the direction of condylar growth was unique in this group. The direction of growth of the dysplastic condyle was more posterior and lateral than that of the contralateral side (Fig 5, *A* [left side] and *E* [right side]). The more posterior component of condyle growth can be appreciated by examining growth vectors from a lateral perspective (data not shown). From the inferior view, the patient in Figure 5, *A*, also showed a significant lateral component of growth at both condyles, with the dysplastic and contralateral sides growing to the left. This subject also developed a cant of the occlusal plane that increased from T0 to T1. Concurrently, the contralateral condyle grew more than the dysplastic side (Fig 5, *B*; right condyle). The patient in Figure 5, *E*, similarly showed lateral growth of the dysplastic condyle.

DISCUSSION

Mandibular growth and remodeling patterns have been extensively studied with tantalum implants[36,37] and histologic sections.[38–43] These studies have shown that no structure or surface of the mandible is a truly stable reference during growth, since all surfaces of bone undergo remodeling over time. Therefore, metallic implants remain the best reference for studying facial growth. Placement is obviously not practical in all patients; for this reason,

Björk[36] developed structural superimposition methods to correctly orient longitudinal time points. These studies, in combination with histologic findings, show extensive apposition along the inferior and outer borders of the symphysis during growth. They also show minimal remodeling at the inner cortical border and lingual surface of the symphysis during adolescent growth. Based on these findings, a U-shaped volume containing the internal structure and the lingual border of the symphysis with erupting tooth buds removed was used as a target for automated, voxel-based 3D registration in this study.

Preliminary studies evaluating 3D registrations have highlighted consistency with both previous findings and new results.[30] The validity of using an automated, regional registration in the mandible to align longitudinal time points was evaluated in a rabbit model.[31] In this study, an affine Procrustes-based registration method was evaluated for accuracy against fiducial metallic implants, showing correspondence at less than 3 voxel widths.[31] Further studies in patients with Apert's syndrome with clinical computed tomography data have shown method errors ranging from 0.4 to 0.8 mm for multiple landmarks.[30] Some structures presumed to be stable in 2-dimensional projections, such as the mandibular canal, may show significant lateral displacement. With the ability to resolve growth changes in 3 planes of space, these methods are a useful approach to study the complex patterns of mandibular growth in patients with congenital and acquired asymmetry.

The deformities in both CFM and dentofacial asymmetry occur in all 3 planes of space and are consequently 3D. Thus, studies with a 3D approach are best suited to study growth and remodeling patterns in these conditions. Previous 3D studies have provided insight into growth of the facial skeleton in patients with CFM.[8,16–18,26] Similarly, studies using CBCT data have also characterized the distinct morphologies of dentofacial asymmetry.[11,33,44] Measuring asymmetric growth patterns in individual bones such as the mandible, however, remains challenging. Changes to the location of landmarks on the mandible can be due to either remodeling or positional displacement. Asymmetric translation of the mandible and changes to the glenoid fossa and cranial base can all contribute to positional or "platform" asymmetry of the mandible, thus confounding the measurement of actual asymmetry. Therefore, true measurement of mandibular asymmetry over time necessitates identifying a reliable reference.

The generalized depiction of mandibular growth in the symmetric adolescent group (Fig 3) is consistent with previous histologic[38,39,43,45] and implant-based[37,41,42,46] studies of mandibular growth and remodeling. However, this control group represented only symmetric orthodontic patients and might not represent "normal" growth in all subjects. The general growth pattern observed during this period is consistent with the overall description of Enlow and Harris[40] of mandibular growth and remodeling, whereby resorption occurs along the inner surface of the ramus, and apposition occurs on the outer surface (Fig 3; right side). Changes along the interior surface of the symphysis were below the limits of detection, correlating well with histologic studies that showed minimal surface remodeling at this location over this period of growth.[38]

Other quantitative measures of mandibular growth based on the uptake of radioactive tracers such as ^{99m}Tc-labeled methylene diphosphate provide a tissue-based and 3D approach to

quantify asymmetric mandibular growth.[47] Planar scintigraphy using ^{99m}Tc-labeled methylene diphosphate, which distributes according to bone blood flow, can be used to evaluate mandibular growth at 1 time point. In the study by Fahey et al,[47] the mean measured ratio of right:left growth determined from ^{99m}Tc-labeled methylene diphosphate uptake was 0.943 ± 0.116 in a symmetric adolescent population. Pripatnanont et al[48] reported a 4.75% ± 1.91% mean difference in isotope uptake in this population. These results are comparable with our observed 1.8% ± 5.7% variation in condylar growth in the control group.

These results support the original hypothesis that mandibular growth rates in patients with dentofacial asymmetry are significantly asymmetric relative to the controls. Authors of previous studies also found a 34.7% ± 15.2% difference in condylar isotope uptake in growing adolescents with dentofacial asymmetry[48]; this is consistent with the 20.2% difference in condylar growth measured in group B in our study. This asymmetry in condylar growth occurred in the same proportion with asymmetry in posterior ramus growth on the hyper-plastic side. In general, the direction of growth paralleled the contralateral side but was greater. These results are based, however, on a short observational window of 2 years. Earlier growth stages have been shown to have more asymmetric growth than later stages, and some of the observed variations can be accounted for by growth stage as well as individual differences in the population.[48]

The clinical implications of such great asymmetries in growth predict a significant increase in mandibular asymmetry over time. Growth asymmetry was greatest (Table II) along the posterior border of the ramus, indicating a strong likelihood for the development of yaw asymmetry in addition to canting during growth.

The results in this study do not support the original hypothesis of asymmetric condylar growth during adolescence in types I and IIA CFM. Growth asymmetry in the CFM group showed no statistically significant difference from the control group (Table II; Fig 7). Furthermore, no relationship between initial morphology or asymmetry and growth pattern was found. The extent to which mandibular proportions are maintained, or become more asymmetric during growth, however, remains controversial. This question is important because impaired growth can increase the severity of the deformity in both jaws over time.[6,14,49] In order to maintain mandibular proportions, the larger side must grow at a proportionally greater rate.[22] Although statistically significant asymmetry was not found in our model, the mean condylar growth rate was slightly less on the dysplastic side (Table II). This slightly lower growth rate is consistent with previous observations of proportional growth. Several studies have measured mandibular growth in patients with CFM types I and IIA during adolescence using a combination of anteroposterior cephalograms, lateral cephalograms, and CBCT data.[8,14,15,18,19] These studies have conflicting results, with some[14,21,49] measuring the increasing cants of the mandible and the maxilla over time in the frontal plane, and others[8,15,18,19,22,50] reporting symmetric growth and no significant changes in facial proportions. Our findings favor the observations of symmetric condylar growth, and the preservation of mandibular proportions over time.

In contrast to growth at the condyle, appreciably less (−33.5% ± 13.2%) apposition along the posterior ramus was observed in the CFM group on the dysplastic side. Growth in this region accounts for lengthening of the mandibular corpus with maturation. Consequently, asymmetric growth along this border would unequally lengthen the mandibular body, an observation in previous studies.[14,15,51] This asymmetry in growth could be explained by the observed decreases in size and activity of the masticatory muscles on the dysplastic side in CFM types I and IIA.[9,10,52,53] Previous electromyography studies have shown that decreased recruitment of masseter muscle fibers on the dysplastic side correlates with reduced apposition at the gonial angle.[10] In addition, reduced sizes of the masseter and temporalis muscles were found to be associated with greater mandibular asymmetry.[52]

The direction of condylar growth, as inferred from superimposed overlays, also differed between sides of the mandible in the CFM group. The overlays in Figure 5 (left side) show a considerable difference in condylar growth direction in the transverse plane. Further analysis of growth vector maps (data not shown) demonstrated a more lateral and posteriorly oriented growth vector on the dysplastic side of the mandible. This was more evident in the type IIA forms of CFM (Fig 5, *A* and E). In contrast, growth in the symmetric controls (Fig 3; left side) was directed parallel to the ramus and perpendicular to the articulating surface. Although limited by only 2 time points, these results indicate potential compensatory growth of the dysplastic side. Examining models of the entire skull during growth, Shibatzaki-Yorozuya et al[18] showed that the condyle maintains its relationship with the articulating surface during growth, despite asymmetric growth of the cranial base. The observed difference in condylar growth direction could therefore be a compensatory response that preserves the condyle-fossa relationship.

The observed differences in mandibular growth pattern between patients with CFM and acquired, noninflammatory forms of dentofacial asymmetry most likely reflect differences in muscle function in the 2 conditions. Previous data support the hypothesis that the size and shape of the mandible in patients with CFM are partly established by functional muscular anatomy.[8–10,52,53] As described, skeletal and neuromuscular defects are present in patients with CFM and ultimately determine growth and remodeling patterns. By adolescence, the underlying neuromuscular anatomy is established, and muscular activity remains at similar levels.[10] Consequently, growth rates are likely to remain proportional on both sides of the jaw during this period as the face lengthens.[40] In patients with CFM, the shape and remodeling of the mandible parallel growth of the surrounding neuromuscular components, which tend to retain established activity patterns over time.[3,10] In contrast, asymmetric mandibular growth in patients with acquired dentofacial asymmetry derives from increased proliferation in the fibrocartilage layer covering the condyle.[5] As a result, growth asymmetry originates at the condyle, which tends to asymmetrically lengthen the ramus and increase mandibular asymmetry over time.

Our findings corroborate these previous results and show that overall mandibular shape and proportion are maintained during adolescent growth in patients with CFM. In contrast, disorders of mandibular growth become more asymmetric over this time period. Together, these data show that both diagnoses have uncertain growth trajectories. For this reason, in

the absence of psychosocial justification, definitive surgical intervention should be postponed until the completion of growth in patients with less severe forms of CFM.

CONCLUSIONS

1. We found no detectable difference in adolescent, presurgical condylar growth between sides in patients with types I and IIA CFM relative to a symmetric orthodontic population. However, significant asymmetry in appositional growth of the posterior ramus was found.
2. In contrast, populations with acquired, noninflammatory dentofacial deformity showed significant asymmetry in growth of both the condyle and the ramus compared with a symmetric orthodontic population.
3. Clinically, these results predict that mandibular proportions are likely to remain constant in patients with mild forms of CFM during adolescent growth, whereas those with disorders of mandibular growth are likely to show increased canting and chin point deviation over time.

Acknowledgments

We thank Sneha Oberoi and Karin Vargervik at the University of California, San Francisco, for helpful insight, assistance, and feedback with this project, and Lucie Macron for invaluable help in developing custom software tools in Slicer for this project.

Supported by an American Association of Orthodontists Foundation Faculty Development Award to R. Christian Solem and a grant from the National Institute of Dental and Craniofacial Research and National Institute of Biomedical Imaging and Bioengineering of the National Institutes of Health (award R01DE024450).

REFERENCES

1. Heike, CL.; Luquetti, DV.; Hing, AV. Craniofacial microsomia overview. In: Pagon, RA.; Adam, MP.; Ardinger, HH.; Wallace, SE.; Amemiya, A.; Bean, LJ., et al., editors. Gene Reviews. Seattle: University of Washington; 1993.
2. Heike CL, Hing AV, Aspinall CA, Bartlett SP, Birgfeld CB, Drake AF, et al. Clinical care in craniofacial microsomia: a review of current management recommendations and opportunities to advance research. Am J Med Genet. 2013; 163C:271–282. [PubMed: 24132932]
3. Vargervik K. Mandibular malformations: growth characteristics and management in hemifacial microsomia and Nager syndrome. Acta Odontol Scand. 1998; 56:331–338. [PubMed: 10066111]
4. Johnston MC, Bronsky PT. Prenatal craniofacial development: new insights on normal and abnormal mechanisms. Crit Rev Oral Biol Med. 1995; 6:25–79. [PubMed: 7632866]
5. Pirttiniemi P, Peltomaki T, Muller L, Luder HU. Abnormal mandibular growth and the condylar cartilage. Eur J Orthod. 2009; 31:1–11. [PubMed: 19164410]
6. Kaban LB. Mandibular asymmetry and the fourth dimension. J Craniofac Surg. 2009; 20(Suppl 1): 622–631. [PubMed: 19182686]
7. Vento AR, LaBrie RA, Mulliken JB. The O.M.E.N.S. classification of hemifacial microsomia. Cleft Palate Craniofac J. 1991; 28:68–76. [PubMed: 1848447]
8. Sarnas KV, Rune B, Aberg M. Maxillary and mandibular displacement in hemifacial microsomia: a longitudinal roentgen stereometric study of 21 patients with the aid of metallic implants. Cleft Palate Craniofac J. 2004; 41:290–303. [PubMed: 15151450]
9. Takashima M, Kitai N, Murakami S, Furukawa S, Kreiborg S, Takada K. Volume and shape of masticatory muscles in patients with hemifacial microsomia. Cleft Palate Craniofac J. 2003; 40:6–12. [PubMed: 12498600]

10. Vargervik K, Miller AJ. Neuromuscular patterns in hemifacial microsomia. Am J Orthod. 1984; 86:33–42. [PubMed: 6588758]
11. Baek C, Paeng JY, Lee JS, Hong J. Morphologic evaluation and classification of facial asymmetry using 3-dimensional computed tomography. J Oral Maxillofac Surg. 2012; 70:1161–1169. [PubMed: 21763045]
12. Boutros S, Shetye PR, Ghali S, Carter CR, McCarthy JG, Grayson BH. Morphology and growth of the mandible in Crouzon, Apert, and Pfeiffer syndromes. J Craniofac Surg. 2007; 18:146–150. [PubMed: 17251854]
13. Kaban LB, Moses MH, Mulliken JB. Correction of hemifacial microsomia in the growing child: a follow-up study. Cleft Palate J. 1986; 23(Suppl 1):50–52. [PubMed: 3545546]
14. Kearns GJ, Padwa BL, Mulliken JB, Kaban LB. Progression of facial asymmetry in hemifacial microsomia. Plast Reconstr Surg. 2000; 105:492–498. [PubMed: 10697151]
15. Polley JW, Figueroa AA, Liou EJ, Cohen M. Longitudinal analysis of mandibular asymmetry in hemifacial microsomia. Plast Reconstr Surg. 1997; 99:328–339. [PubMed: 9030137]
16. Rune B, Sarnas KV, Selvik G, Jacobsson S. Roentgen stereometry with the aid of metallic implants in hemifacial microsomia. Am J Orthod. 1983; 84:231–247. [PubMed: 6577796]
17. Rune B, Selvik G, Sarnas KV, Jacobsson S. Growth in hemifacial microsomia studied with the aid of roentgen stereophotogrammetry and metallic implants. Cleft Palate J. 1981; 18:128–146. [PubMed: 6939508]
18. Shibazaki-Yorozuya R, Yamada A, Nagata S, Ueda K, Miller AJ, Maki K. Three-dimensional longitudinal changes in craniofacial growth in untreated hemifacial microsomia patients with conebeam computed tomography. Am J Orthod Dentofacial Orthop. 2014; 145:579–594. [PubMed: 24785922]
19. Kusnoto B, Figueroa AA, Polley JW. A longitudinal three-dimensional evaluation of the growth pattern in hemifacial microsomia treated by mandibular distraction osteogenesis: a preliminary report. J Craniofac Surg. 1999; 10:480–486. [PubMed: 10726500]
20. Kaban LB, Moses MH, Mulliken JB. Surgical correction of hemifacial microsomia in the growing child. Plast Reconstr Surg. 1988; 82:9–19. [PubMed: 3289066]
21. Kaban LB, Padwa BL, Mulliken JB. Surgical correction of mandibular hypoplasia in hemifacial microsomia: the case for treatment in early childhood. J Oral Maxillofac Surg. 1998; 56:628–638. [PubMed: 9590345]
22. Shetye PR, Grayson BH, Mackool RJ, McCarthy JG. Long-term stability and growth following unilateral mandibular distraction in growing children with craniofacial microsomia. Plast Reconstr Surg. 2006; 118:985–995. [PubMed: 16980861]
23. Bartlett SP. No evidence for long-term effectiveness of early osteo-distraction in hemifacial microsomia. Plast Reconstr Surg. 2010; 125:1567–1568. [PubMed: 20440178]
24. Grummons DC, Kappeyne van de Coppello MA. A frontal asymmetry analysis. J Clin Orthod. 1987; 21:448–465. [PubMed: 3476493]
25. Figueroa AA, Pruzansky S. The external ear, mandible and other components of hemifacial microsomia. J Maxillofac Surg. 1982; 10:200–211. [PubMed: 6961179]
26. Kaban LB, Mulliken JB, Murray JE. Three-dimensional approach to analysis and treatment of hemifacial microsomia. Cleft Palate J. 1981; 18:90–99. [PubMed: 6939510]
27. Baccetti T, Franchi L, McNamara JA Jr. An improved version of the cervical vertebral maturation (CVM) method for the assessment of mandibular growth. Angle Orthod. 2002; 72:316–323. [PubMed: 12169031]
28. Nguyen T, Cevidanes LH, George W. Validation of 3D mandibular regional superimposition methods for growing patients [abstract]. J Dent Res. 2014; 93(Spec Iss A):784.
29. Bland JM, Altman DG. Comparing methods of measurement: why plotting difference against standard method is misleading. Lancet. 1995; 346:1085–1087. [PubMed: 7564793]
30. Krarup S, Darvann TA, Larsen P, Marsh JL, Kreiborg S. Three-dimensional analysis of mandibular growth and tooth eruption. J Anat. 2005; 207:669–682. [PubMed: 16313399]
31. Kim I, Oliveira ME, Duncan WJ, Cioffı I, Farella M. 3D assessment of mandibular growth based on image registration: a feasibility study in a rabbit model. Biomed Res Int. 2014; 2014:276128. [PubMed: 24527442]

32. Styner M, Oguz I, Xu S, Brechbuhler C, Pantazis D, Levitt JJ, et al. Framework for the statistical shape analysis of brain structures using SPHARM-PDM. Insight J. 2006; (1071):242–250. [PubMed: 21941375]
33. Alhadidi A, Cevidanes LH, Paniagua B, Cook R, Festy F, Tyndall D. 3D quantification of mandibular asymmetry using the SPHARM-PDM tool box. Int J Comput Assist Radiol Surg. 2012; 7:265–271. [PubMed: 22089896]
34. Fox, J. Applied regression analysis and generalized linear models. 3rd. Thousand Oaks, Calif: SAGE Publications; 2015.
35. Snijders, TA.; Bosker, RJ. Multilevel analysis: an introduction to basic and advanced multilevel modeling. 2nd. Thousand Oaks, Calif: SAGE Publications; 2012.
36. Bjork A. Variations in the growth pattern of the human mandible: longitudinal radiographic study by the implant method. J Dent Res. 1963; 42(Pt 2):400–411. [PubMed: 13971295]
37. Bjork A. Prediction of mandibular growth rotation. Am J Orthod. 1969; 55:585–599. [PubMed: 5253957]
38. Martinez-Maza C, Rosas A, Nieto-Diaz M. Postnatal changes in the growth dynamics of the human face revealed from bone modelling patterns. J Anat. 2013; 223:228–241. [PubMed: 23819603]
39. Enlow DH, Harris DB. A study of postnatal growth of the human mandible. Am J Orthod. 1964; 50:25–50.
40. Enlow, DH.; Hans, MG. Essentials of facial growth. 2nd. Ann Arbor, Mich: Needham Press; 2008.
41. Gu Y, McNamara JA Jr. Cephalometric superimpositions. Angle Orthod. 2008; 78:967–976. [PubMed: 18947269]
42. Bjork A, Skieller V. Normal and abnormal growth of the mandible. A synthesis of longitudinal cephalometric implant studies over a period of 25 years. Eur J Orthod. 1983; 5:1–46. [PubMed: 6572593]
43. Enlow DH. A morphogenetic analysis of facial growth. Am J Orthod. 1966; 52:283–299. [PubMed: 5217789]
44. Cevidanes LH, Alhadidi A, Paniagua B, Styner M, Ludlow J, Mol A, et al. Three-dimensional quantification of mandibular asymmetry through cone-beam computerized tomography. Oral Surg Oral Med Oral Pathol Oral Radiol Endod. 2011; 111:757–770. [PubMed: 21497527]
45. Hans MG, Enlow DH, Noachtar R. Age-related differences in mandibular ramus growth: a histologic study. Angle Orthod. 1995; 65:335–340. [PubMed: 8526292]
46. Skieller V, Bjork A, Linde-Hansen T. Prediction of mandibular growth rotation evaluated from a longitudinal implant sample. Am J Orthod. 1984; 86:359–370. [PubMed: 6594058]
47. Fahey FH, Abramson ZR, Padwa BL, Zimmerman RE, Zurakowski D, Nissenbaum M, et al. Use of (99m)Tc-MDP SPECT for assessment of mandibular growth: development of normal values. Eur J Nucl Med Mol Imaging. 2010; 37:1002–1010. [PubMed: 20033153]
48. Pripatnanont P, Vittayakittipong P, Markmanee U, Thongmak S, Yipintsoi T. The use of SPECT to evaluate growth cessation of the mandible in unilateral condylar hyperplasia. Int J Oral Maxillofac Surg. 2005; 34:364–368. [PubMed: 16053843]
49. Mulliken JB, Kaban LB. Analysis and treatment of hemifacial microsomia in childhood. Clin Plast Surg. 1987; 14:91–100. [PubMed: 3816041]
50. Sarnas KV, Pancherz H, Rune B, Selvik G. Hemifacial microsomia treated with the Herbst appliance. Report of a case analyzed by means of roentgen stereometry and metallic implants. Am J Orthod. 1982; 82:68–74. [PubMed: 6961779]
51. Ongkosuwito EM, van Vooren J, van Neck JW, Wattel E, Wolvius EB, van Adrichem N, et al. Changes of mandibular ramal height, during growth in unilateral hemifacial microsomia patients and unaffected controls. J Craniomaxillofac Surg. 2013; 41:92–97. [PubMed: 22789870]
52. Huisinga-Fischer CE, Zonneveld FW, Vaandrager JM, Prahl-Andersen B. Relationship in hypoplasia between the masticatory muscles and the craniofacial skeleton in hemifacial microsomia, as determined by 3-D CT imaging. J Craniofac Surg. 2001; 12:31–40. [PubMed: 11314185]
53. Heude E, Rivals I, Couly G, Levi G. Masticatory muscle defects in hemifacial microsomia: a new embryological concept. Am J Med Genet A. 2011; 155A:1991–1995. [PubMed: 21744489]

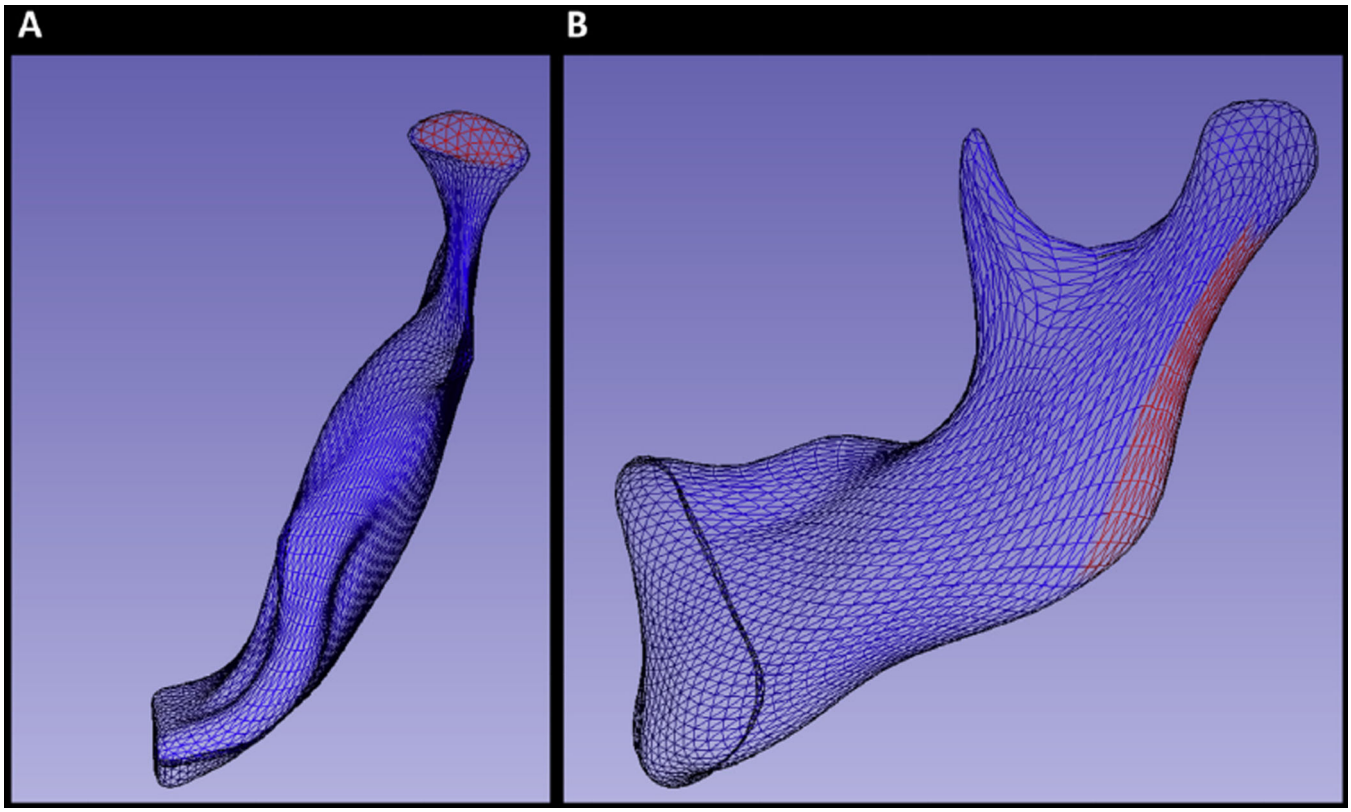

Fig 1.

Methods for regional growth measurement. Shape correspondence analysis parameterizes each hemimandibular surface into mesh points (*blue wire frame*) mapped to a spherical coordinate system. **A**, Region of 61 mesh points was selected by defining a 4-point radius centered on the superior articulating surface of the condyle; **B**, region of 91 mesh points was defined by a 5-point radius centered on the posterior ramus. These 2 regions were automatically selected in each mandible based on the corresponding region of shape in each subject.

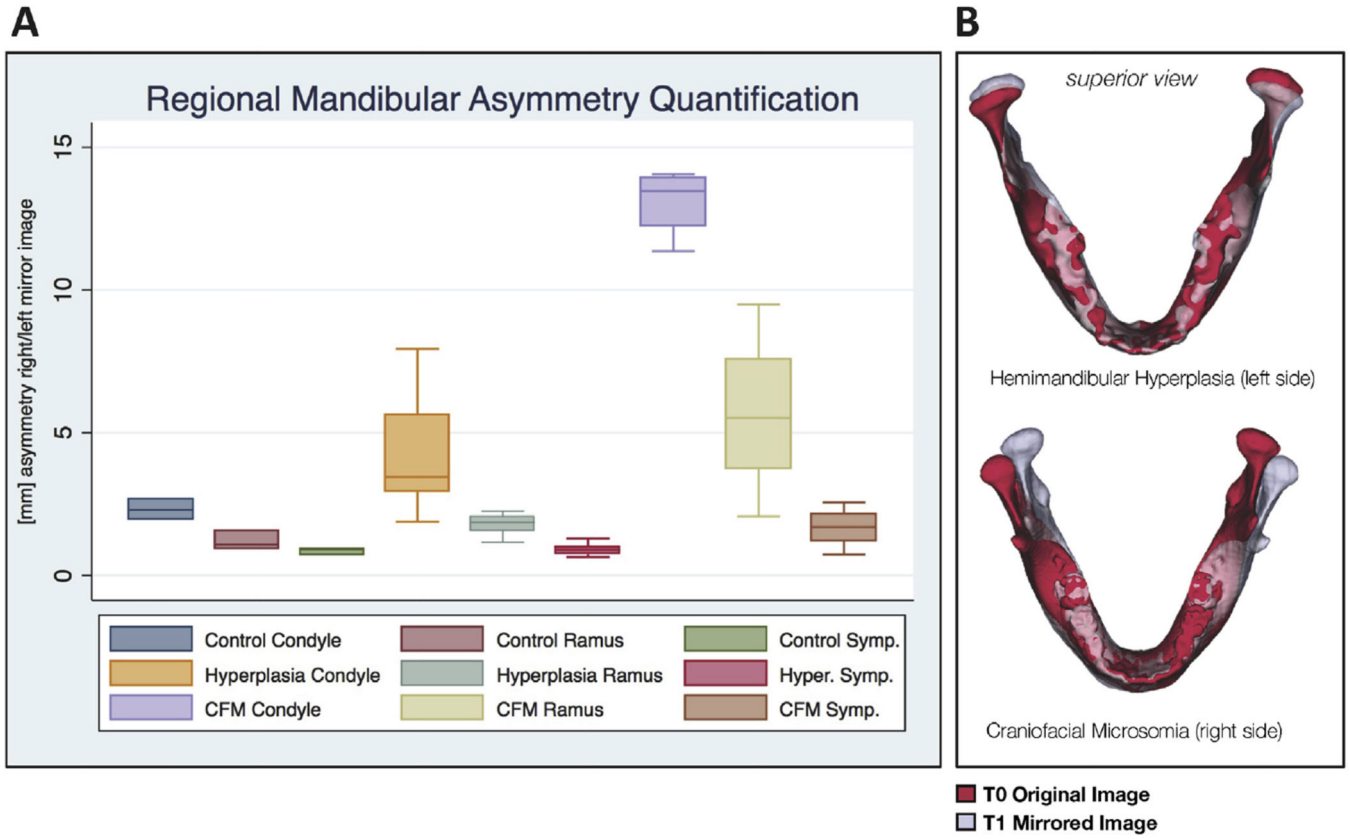

Fig 2.

Initial mandibular asymmetry analysis at T0. Mandibular asymmetry was characterized at T0 by comparing each mandible with its mirror image. **A**, The degree of displacement between corresponding structures on the right and left sides is shown. The shape regions selected included the condyle, ramus, and symphysis. Box plots are shown for each population and region indicating the median, 25th, 75th percentile (*box*), and range of measurements (*whiskers*). **B**, To quantify asymmetry over the selected regions, the entire mandibular shape at T0 was reflected in the sagittal plane, from right to left. The original mandible is shown in *red*, and the mirror image is shown in *white* (superior view). The mirror image of the mandible was registered on the original at the symphysis. Deviations between the *red* and *white* images reflect differences in shape between the right and left sides. Patients with hemimandibular hyperplasia (*top*) and craniofacial microsomia (*bottom*) are shown, demonstrating both vertical and transverse asymmetries.

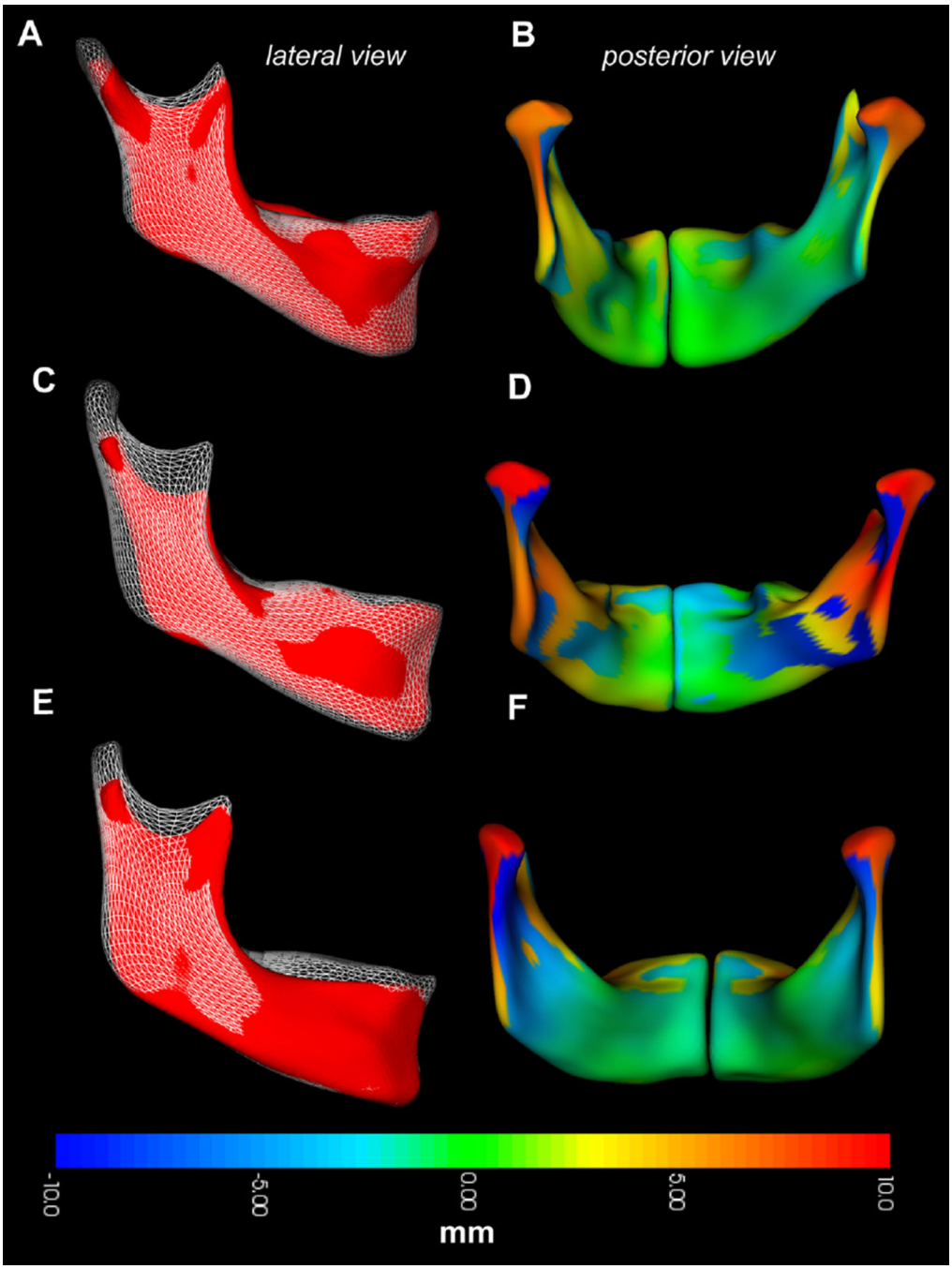

Fig 3.

Regional growth in the control group. Regional growth of the mandible is shown in the control group as an overlay of registered longitudinal mandibular surfaces of the same subject. Three subjects are shown from a lateral perspective, with T0 shown as a *red surface*, and T1 shown as a *white mesh overlay* (lateral views: **A, C**, and **E**). Growth in the same 3 subjects is measured as the displacement between corresponding points, show as a millimeter color scale in **B, D**, and **F**. Separate right and left hemimandibles required for shape correspondence analysis are fused into a single image. On the colored surfaces,

outward apposition is shown in *yellow-red* color. Inward resorption is shown in *turquoise-blue* color. Areas in *green* had undetectable changes. **A** and **B**, Mandibular growth in a boy (patient A2) from T0 (age, 10.7 years) to T1 (12.4 years). **C** and **D**, Mandibular growth in a girl (patient A1) from T0 (age, 12.3 years) to T1 (14.2 years). **E** and **F**, Mandibular growth in a girl (patient A3) from T0 (age, 10.8 years) to T1 (13.8 years).

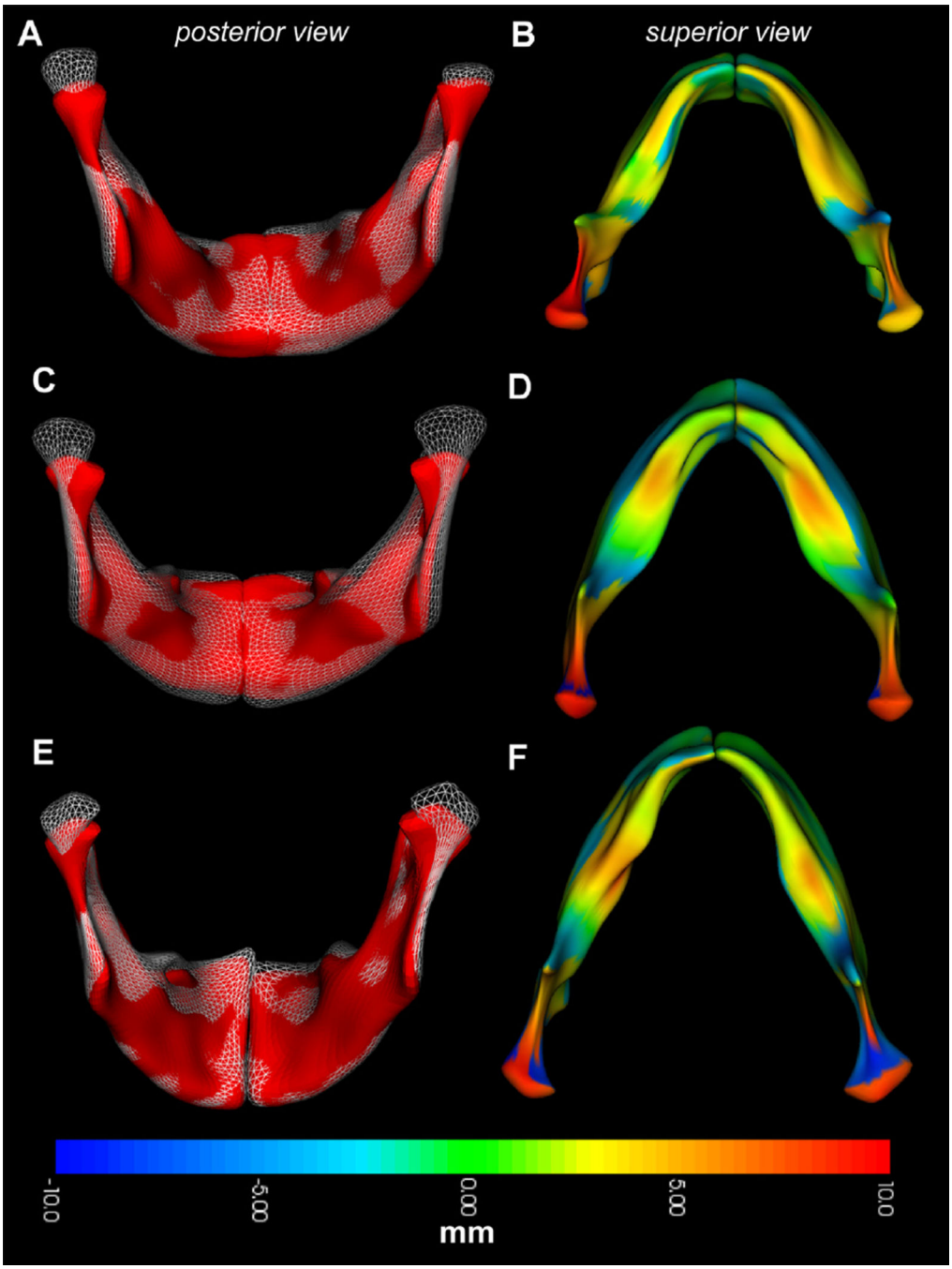

Fig 4.

Asymmetric growth in dentofacial deformity. Regional growth of the mandible is shown as an overlay of registered longitudinal time points (posterior views: **A, C**, and **E**) and millimeter color scale indicating displacement of corresponding mesh points (superior views: **B, D**, and **F**). **A** and **B**, Mandibular growth in a girl (patient B9) with left-sided hyperplasia measured from T0 (age, 11.6 years) (*red surface*) to T1 (13.3 years) (*white mesh overlay*). **C** and **D**, Mandibular growth in a girl (patient B1) with left-sided hyperplasia at T0 (age, 12.0 years) (*red surface*) to T1 (15.1 years) (*white mesh overlay*). **E** and **F**, Mandibular

growth in a girl (patient B10) with right-sided hyperplasia from T0 (age, 12.3 years) to T1 (14.2 years).

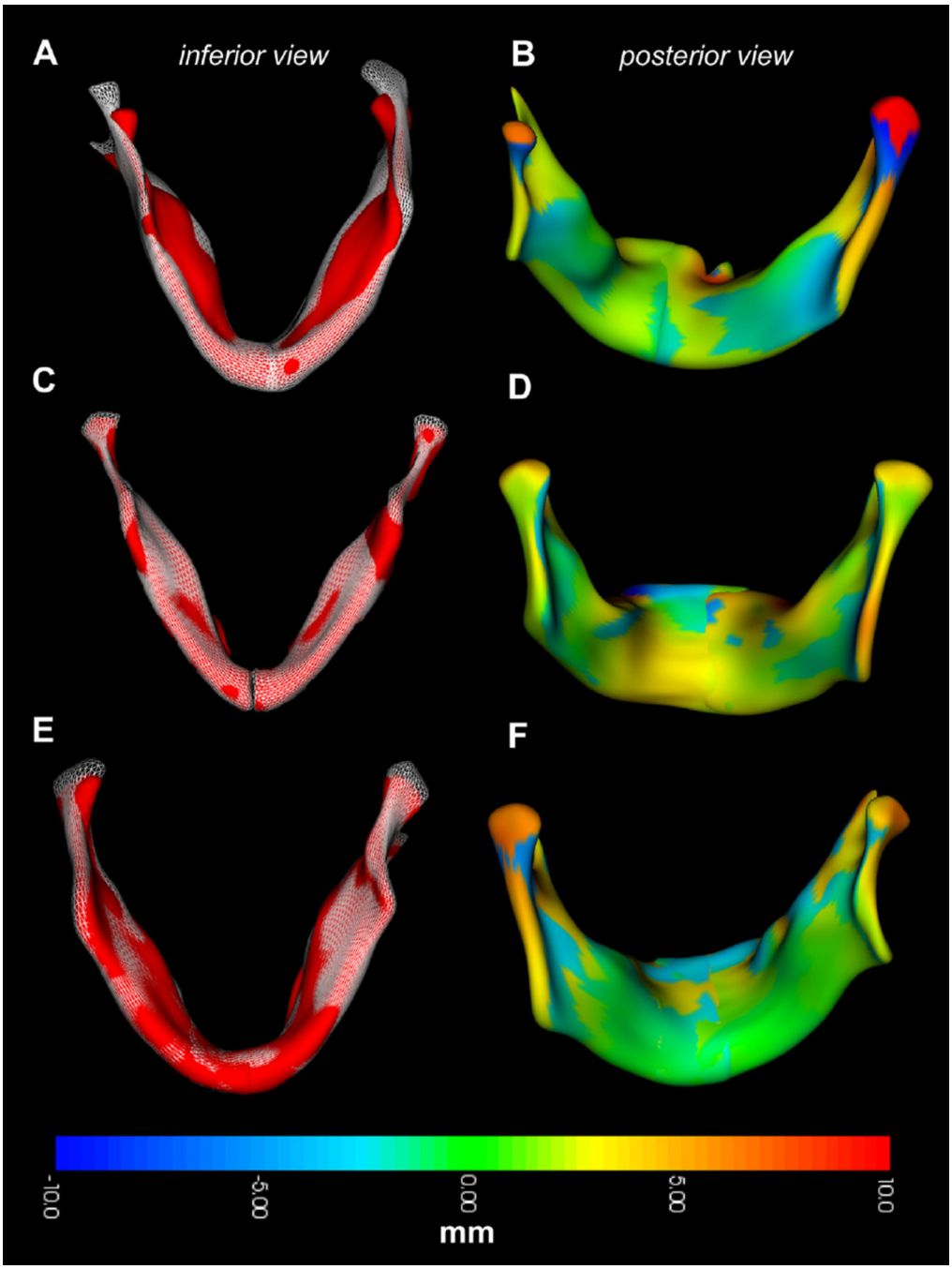

Fig 5.

Regional growth in CFM. Regional growth of the mandible is depicted as an overlay of longitudinal time points (inferior views: **A, C**, and **E**) and millimeter color scale (posterior views: **B, D**, and **F**) in 3 subjects diagnosed with CFM or OAV. **A** and **B**, Mandibular growth in a boy (patient C5) with type IIA OAV spectrum disorder and dysplasia of the left side, measured from T0 (age, 11.4 years) (*red surface*) to T1 (15.1 years) (*white mesh overlay*). Condylar and posterior ramus growth are greater on the right side (*red color, right side*). **C** and **D**, Mandibular growth in a girl (patient C3) with type I CFM with dysplasia of the left

side, measured from T0 (age, 9.3 years) (*red surface*) to T1 (10.8 years) (*white mesh overlay*). Posterior ramus growth is greater on the left side (*red-orange color*). **E** and **F**, Mandibular growth in a girl (patient C1) with type IIA OAV and dysplasia of the right side measured from T0 (age, 11.8 years) (*red surface*) to T1 (13.8 years) (*white mesh overlay*). Observe the difference in posterior ramus growth between the left (*red-orange*) and right (*yellow*) sides.

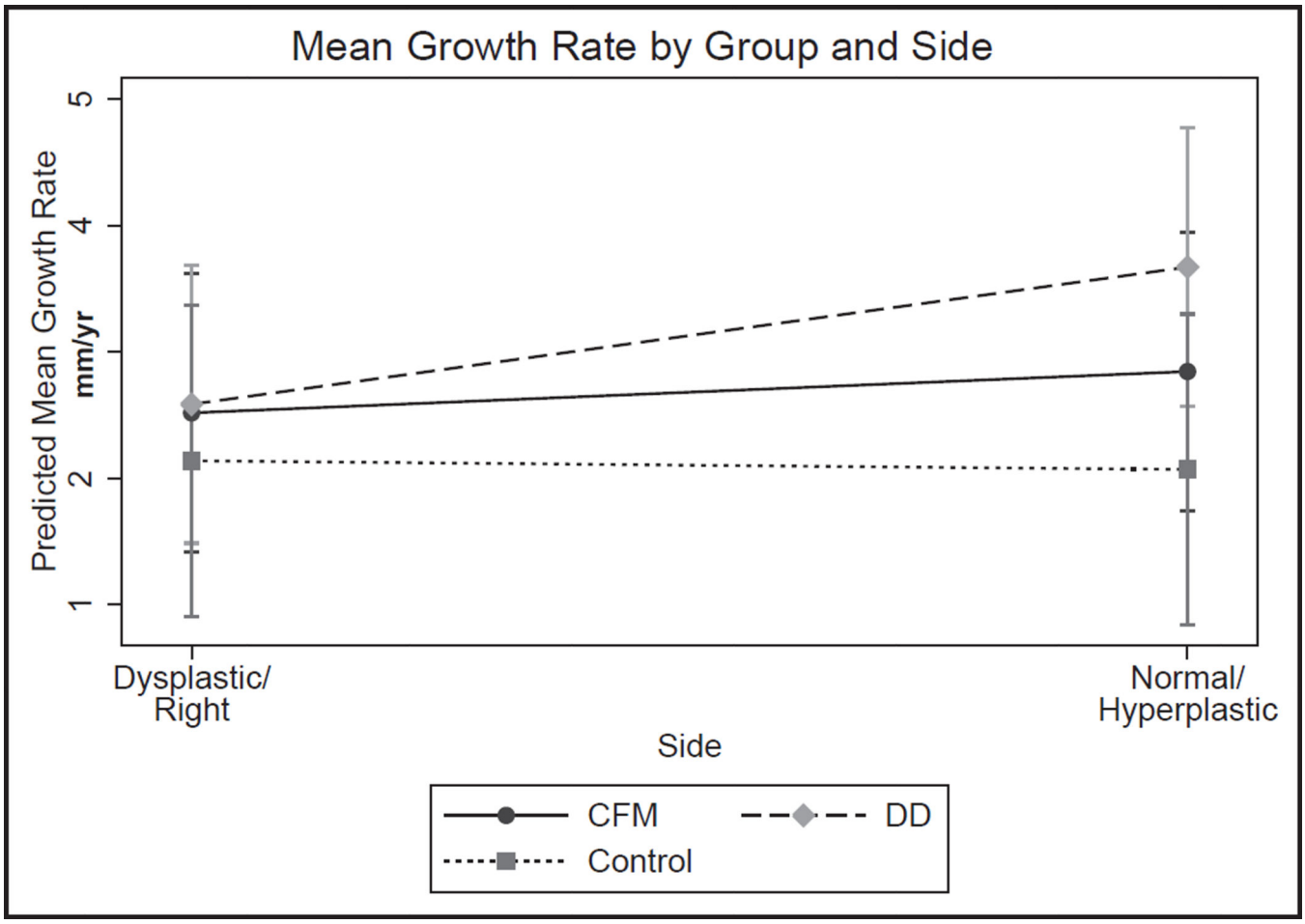

Fig 6.

Predicted mean growth rate by side. Overall differences in the predicted growth rate between sides of the mandible are shown for the CFM group, the dentofacial deformity group (*DD*), and the control. Measurements are averaged over all regions on the particular side of the mandible. In the CFM group, the dysplastic side shows an overall lower mean growth rate than the “normal” side. In the dentofacial deformity group, the hyperplastic side has the overall highest mean growth rate and the greatest difference between sides. A detectable but statistically insignificant difference in growth rate was measured in the control group.

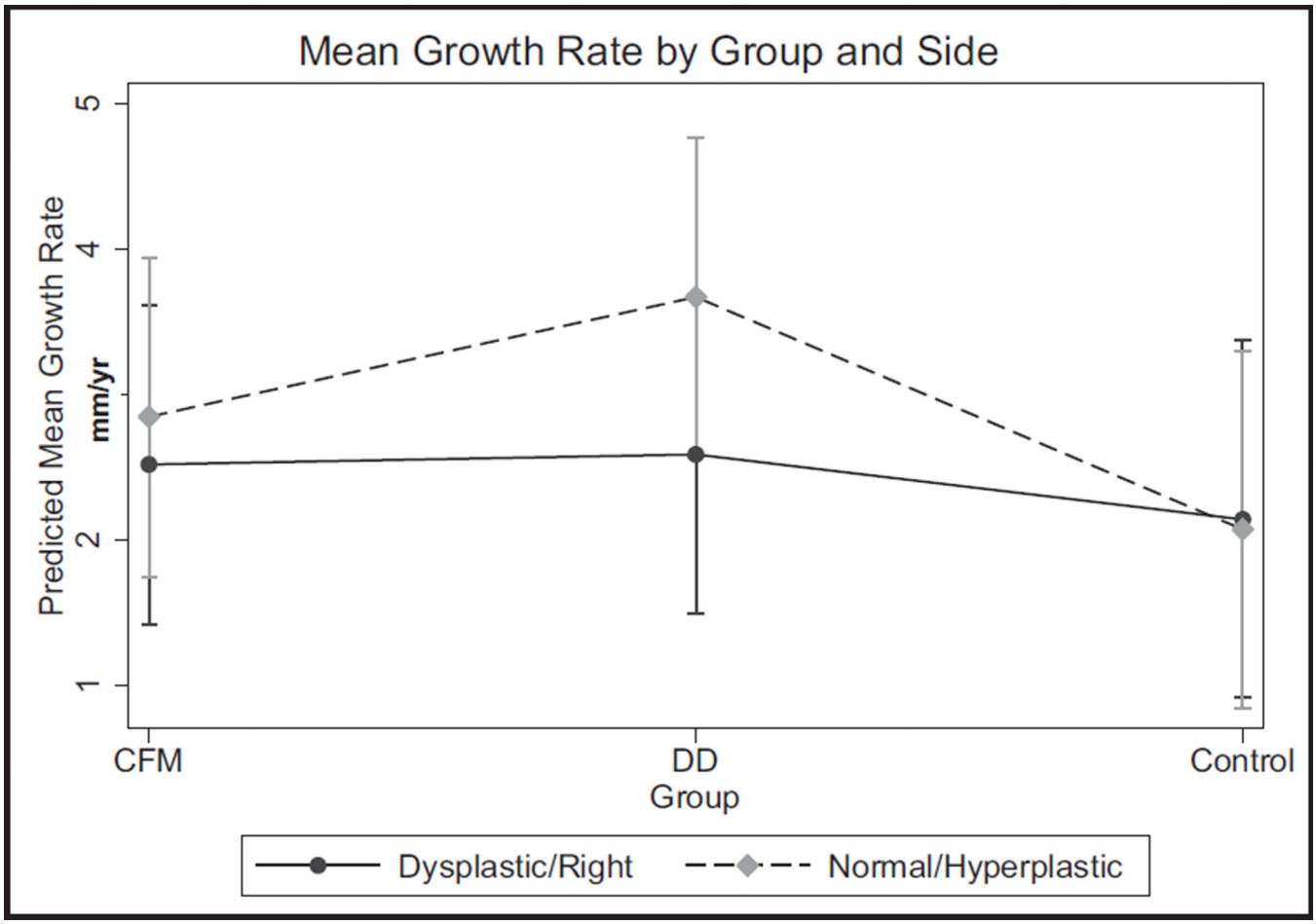

Fig 7.

Predicted mean growth rate by group. Differences in the predicted growth asymmetry by group are shown for the 3 groups. Both the CFM group and the dentofacial deformity group (*DD*) showed a difference in mean growth between sides, with the dentofacial dentofacial deformity group showing the largest difference. The overall predicted mean mandibular growth rate on the hyperplastic side in the dentofacial deformity group is greater than the growth rates on both sides of the mandible in the other 2 groups.

Table I

Sample population characteristics

Patient	Diagnosis	T0 age (y)	T1 age (y)	Sex	CVM stage at T0
Group A, symmetric controls					
A1		12.3	14.2	F	III
A2		10.7	12.4	M	I
A3		10.8	13.8	F	II
A4		12.2	14.8	F	III
A5		12.7	15.2	F	III
A6		12.9	14.9	F	III
A7		13.0	15.0	F	II
A8		14.8	17.0	M	III
A9		13.5	15.2	M	II
A10		12.3	14.2	M	III
Mean		12.5	14.7		
Group B, dentofacial asymmetry					
B1	Hyperplasia left side	12.0	15.1	F	II
B2	Hyperplasia left side	12.1	14.0	F	II
B3	Hyperplasia right side	10.6	12.8	M	I
B4	Hyperplasia left side	10.3	12.3	F	II
B5	Hyperplasia right side	8.9	11.4	F	II
B6	Hyperplasia right side, prognathic	16.8	20.3	M	III
B7	Hyperplasia left side, canting	14.0	16.1	M	III
B8	Hyperplasia left side, canting	9.8	13.2	M	I
B9	Hyperplasia left side	11.6	13.3	F	II
B10	Hyperplasia right side, canting	12.3	14.2	F	III

Patient	Diagnosis	T0 age (y)	T1 age (y)	Sex	CVM stage at T0
Mean		11.8	14.2		
Group C, CFM					
C1	OAV spectrum disorder, type IIA right CFM	11.8	13.8	F	II
C2	Type I left CFM	8.0	8.6	M	I
C3	Type I left CFM	9.3	10.8	F	II
C4	Type IIA left CFM	16.3	20.0	M	IV
C5	Type IIA left OAV	11.4	15.1	M	I
C6	Type IIA right Goldenhar's syndrome	8.3	8.9	F	I
C7	Type I left CFM	16.4	17.2	M	III
C8	Type I left CFM	13.7	15.4	M	II
C9	Type I right CFM	16.6	19.9	F	IV
Mean		12.4	14.4		

CFM type and OAV according to the classifications of Pruzansky-Kaban.[25,26] T0 and T1 ages are the time points of radiographic analysis before surgery.

F, Female; *M*, male.

Table II

Regional mean growth measurements over the condyle and posterior ramus, as described in Figure 1

	Condyle				Posterior ramus			
Group	**Mean growth side 1 (mm/y)**	**Mean growth side 2 (mm/y)**	**Mean % Δ**	***P* value**	**Mean growth side 1 (mm/y)**	**Mean growth side 2 (mm/y)**	**Mean % Δ**	***P* value**
A, control	3.8 ± 1.1	3.9 ± 0.9	−1.81		2.6 ± 1.1	2.6 ± 1.2	−0.2	
B, dentofacial asymmetry	4.0 ± 1.2	4.8 ± 1.6	−20.2	<0.001	3.2 ± 1.3	4.6 ± 1.7	−38.3	<0.001
C, craniofacial microsomia	3.3 ± 1.9	3.6 ± 2.6	−3.1	0.47	2.6 ± 1.7	3.6 ± 2.4	−33.5	<0.001

Mean growth indicates the regional means and standard deviations of growth measurements in the group on the indicated side of the mandible. In group A, the difference is defined as the mean growth of the right side 1 (first column) minus the left side 2 (second column). In group B, this difference is defined as the mean growth of the “unaffected” side 1 minus the hyperplastic side 2. In group C, it is defined as the mean growth of the dysplastic side 1 minus the “normal” side 2.

Mean % Δ, Mean percentage of growth asymmetry in each group. Growth asymmetry values were tested against group A for significant difference.